Study of Conventional Control Algorithms for PV-Based Grid-Connected Microgrid

Nikita Gupta, Rachana Garg and Parmod Kumar

Abstract This paper evaluates four conventional algorithms of determining the compensating current for a PV inverter used for integrating PV array with grid. The algorithms studied are synchronous reference frame (SRF) theory, unit template, instantaneous reactive power (IRP) theory, and conductance Fryze. The system has been modeled and implemented in MATLAB along with Simulink toolbox. Simulation results of the performance of four algorithms are presented and analyzed for control of power flow and harmonics reduction in PV-based grid-connected microgrid system.

Keywords Photovoltaic array · Microgrid · Control algorithms · PV inverter

1 Introduction

In the last two decades, awareness of consumers about green technologies, environment concerns, and depletion of the stock of fossil fuel has forced the planners and grid designers to explore the renewable energy sources and alternative sources viz. Photovoltaic (PV) Cell, wind turbine generator, storage battery, microhydropower. In India due to abundance of sunlight, solar energy is gaining lots of importance. The output of PV cell is DC voltage and integration with conventional AC microgrid requires semiconductor inverters along with their controllers. Power generated from PV modules faces the problems concerning power quality like waveform distortion, unbalance, and fluctuations in voltage and/or current.

Nikita Gupta (✉) · Rachana Garg
Delhi Technological University, Delhi, India
e-mail: guptanikita08@gmail.com

Rachana Garg
e-mail: rachana16100@yahoo.co.in

Parmod Kumar
Maharaja Agrasen Institute of Technology, Delhi, India
e-mail: pramodk2003@gmail.com

R. Singh and S. Choudhury (eds.), *Proceeding of International Conference on Intelligent Communication, Control and Devices*, Advances in Intelligent Systems and Computing 479, DOI 10.1007/978-981-10-1708-7_25

So, utilization of PV module efficiently needs output voltage and current to be tracked and optimized using appropriate control algorithm [1, 2]. Inverter plays a vital role for processing, control, and synchronization of generated power with grid. Performance of PV inverter is based on active, reactive, and harmonic current estimation. Accuracy of performance is decided by control algorithm. Several control schemes have been designed and reported in literature [3, 4]. In this paper, the author(s) have discussed and compared synchronous reference frame (SRF) theory, unit template, instantaneous reactive power (IRP) theory, and conductance Fryze based control algorithms. MATLAB and Simulink toolbox-based simulation analysis is presented for demonstration of effectiveness of these control techniques for PV-based grid-connected microgrid system.

2 Design of Control Algorithms

The different control algorithms are applied in the closed-loop control of PV inverter to generate gating pulse signals. Difference lies in the sensed parameters and their processing to generate the reference current signal for gating pulse generation. Once the reference signals (i_{ra}*, i_{rb}*, i_{rc}*) are obtained, they are processed with measured currents using hysteresis current controller (HCC). HCC generates the six gating pulse signal for the PV inverter. The proposed algorithms are implemented on a 10 kW PV-based grid connected microgrid as shown in Fig. 1 [5].

2.1 Synchronous Reference Frame Theory

In the SRF theory-based algorithm, sensed i_{la}, i_{lb} and i_{lc}; V_{terma}, V_{termb} and V_{termc} and v_{dc} are fed to controller for extracting the reference currents [6]. SRFT algorithm

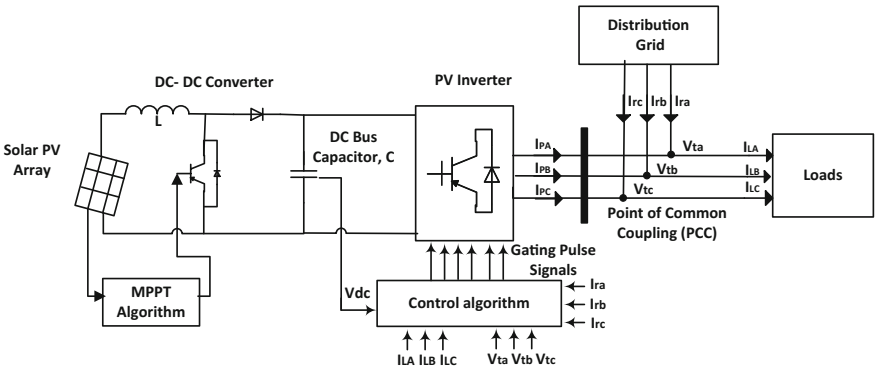

Fig. 1 Schematic diagram of PV-based grid-connected microgrid

uses Park's transformation to reduce three-phase AC quantities to two DC quantities for simplified calculations, given by Eqs. (1) and (2):

$$i_d = \frac{2}{3}\left(i_a \mathrm{Re}\{e^{i\alpha}\} + i_b \mathrm{Re}\{e^{i\beta}\} + i_c \mathrm{Re}\{e^{i\gamma}\}\right) \tag{1}$$

$$i_q = \frac{2}{3}\left(i_a \mathrm{Im}\{e^{i\alpha}\} + i_b \mathrm{Im}\{e^{i\beta}\} + i_c \mathrm{Im}\{e^{i\gamma}\}\right) \tag{2}$$

where α is (ωt), β is ($\alpha - 2\pi/3$), and γ is ($\alpha + 2\pi/3$). The two DC quantities, I_d (d-axis) current and I_q (q-axis) current are used to control the real and reactive power respectively. The PV inverter generated AC supply has to be synchronized with the grid supply before connection. The generated signals are synchronized with the grid using phase-locked loop (PLL). A PI controller is used for the DC bus voltage regulation. Output of PI is loss current (i_{loss}) component of power of system. To generate the reference currents inverse Park's transformation is carried out using Eqs. (3–5)

$$i^*_{\mathrm{ra}} = \left(i^*_d \mathrm{Re}\{e^{i\alpha}\} + i^*_q \mathrm{Im}\{e^{i\alpha}\}\right) \tag{3}$$

$$i^*_{\mathrm{rb}} = \left(i^*_d \mathrm{Re}\{e^{i\beta}\} + i^*_q \mathrm{Im}\{e^{i\beta}\}\right) \tag{4}$$

$$i^*_{\mathrm{rc}} = \left(i^*_d \mathrm{Re}\{e^{i\gamma}\} + i^*_q \mathrm{Im}\{e^{i\gamma}\}\right) \tag{5}$$

2.2 Unit Template Algorithm

In the unit template control algorithm, sensed inputs $i_{\mathrm{la}}, i_{\mathrm{lb}}$ and i_{lc}; $i_{\mathrm{ra}}, i_{\mathrm{rb}}$ and i_{rc}; V_{terma}, V_{termb} and V_{termc} and v_{dc} are fed to controller for extracting the reference currents [7]. Unit vectors in phase and in quadrature with terminal voltages are calculated using terminal voltage amplitude (V_{term}) as shown in Eqs. (6–8)

$$V_{\mathrm{term}} = \sqrt{\frac{2}{3}\left(V^2_{\mathrm{terma}} + V^2_{\mathrm{termb}} + V^2_{\mathrm{termc}}\right)} \tag{6}$$

$$p_a = v_{\mathrm{sa}}/v_{\mathrm{term}}, p_b = v_{\mathrm{sb}}/v_{\mathrm{term}}, p_c = v_{\mathrm{sc}}/v_{\mathrm{term}} \tag{7}$$

$$q_a = p_c - p_b/\sqrt{3}, q_b = p_a/\sqrt{2} + (p_b - p_c)/\sqrt{6}, q_c = -p_a/\sqrt{2} + (p_b - p_c)/\sqrt{6} \tag{8}$$

The unit vectors obtained are used to obtain the active load power and reactive load power given by Eqs. (9) and (10).

$$P = V_{\text{term}} \times (p_a * i_{\text{la}} + p_b * i_{\text{lb}} + p_c * i_{\text{lc}}) \tag{9}$$

$$Q = V_{\text{term}} \times (q_a * i_{\text{la}} + q_b * i_{\text{lb}} + q_c * i_{\text{lc}}) \tag{10}$$

The total load power calculated has two components, DC component (P_{dc}, Q_{dc}) and oscillating AC component (P_{ac}, Q_{ac}). AC component is harmonic component, which is removed using filter and active (I_{pf}) and reactive (I_{qf}) load current components are obtained. PV inverter is used to supply active load power as well as losses to maintain the unity power factor. PI controller helps in DC bus voltage regulation. Output of PI is loss current (i_{loss}) component of power of system. The unit vectors are then used to calculate the active and reactive components of reference grid currents, using Eqs. (11) and (12)

$$i_{\text{pra}} = p_a \times \left(i_{\text{pf}} + i_{\text{loss}}\right), i_{\text{prb}} = p_b \times \left(i_{\text{pf}} + i_{\text{loss}}\right), i_{\text{prc}} = p_c \times \left(i_{\text{pf}} + i_{\text{loss}}\right) \tag{11}$$

$$i_{\text{qra}} = q_a \times \left(i_{\text{qf}} + i_{\text{acq}}\right), i_{\text{qrb}} = q_b \times \left(i_{\text{qf}} + i_{\text{acq}}\right), i_{\text{qrc}} = q_c \times \left(i_{\text{qf}} + i_{\text{acq}}\right) \tag{12}$$

The addition of the above two components provide the total reference currents.

2.3 Instantaneous Reactive Power Theory

In the IRP theory-based algorithm, sensed $i_{\text{la}}, i_{\text{lb}}$ and i_{lc}; $v_{\text{la}}, v_{\text{lb}}$ and v_{lc} and v_{dc} are fed to controller for extracting the reference currents [8]. In IRPT, active and reactive power are calculated in α–β frame using Clarke's transformation given by Eqs. (13) and (14)

$$v_\alpha + jv_\beta = \sqrt{\frac{2}{3}}\left(v_a + v_b e^{\frac{j2\Pi}{3}} + v_c e^{-\frac{j2\Pi}{3}}\right) \tag{13}$$

$$i_\alpha + ji_\beta = \sqrt{\frac{2}{3}}\left(i_a + i_b e^{\frac{j2\Pi}{3}} + i_c e^{-\frac{j2\Pi}{3}}\right) \tag{14}$$

The estimated active power and reactive power are given by Eqs. (15) and (16).

$$P = v_\alpha i_\alpha + v_\beta i_\beta = P_{\text{dc}} + P_{\text{ac}} \tag{15}$$

$$Q = v_\alpha i_\beta - v_\beta i_\alpha = Q_{\text{dc}} + Q_{\text{ac}} \tag{16}$$

Calculated active and reactive power consists of fundamental component (P_{dc}, Q_{dc}) and harmonic component (P_{ac}, Q_{ac}). To remove the harmonic component, these instantaneous powers are passed through low-pass filter. Filter allows only fundamental signal to pass through. The reference currents are then obtained from

fundamental power signals which are in α, β frame. Inverse Clarke's transform is used to recover three-phase AC quantities of reference currents.

2.4 Conductance Fryze Algorithm

In the conductance Fryze control algorithm, sensed i_{la}, i_{lb} and i_{lc} and v_{terma}, v_{termb} and v_{termc} are fed to controller for extracting the reference currents [9]. In conductance Fryze algorithm, the average conductance value (G_{avg}) is calculated form three-phase terminal voltages and load currents using Eq. (17).

$$G_{avg} = (v_{terma} i_{la} + v_{termb} i_{lb} + v_{termc} i_{lc})/(v_{terma}^2 + v_{termb}^2 + v_{termc}^2) \tag{17}$$

The calculated value of average conductance value is passed through low-pass filter (LPF) that allows only fundamental signal to pass through. PI controller helps in DC bus voltage regulation, generating a loss component (G_{loss}) which is provided by PV inverter to the system. The net conductance G is obtained using Eq. (18)

$$G = G_{avg} + G_{loss} \tag{18}$$

Reference currents are obtained by multiplying the net conductance with the terminal voltages as shown in Eq. (19).

$$i_{ra}^* = G \times v_{terma}, i_{rb}^* = G \times v_{termb}, i_{rc}^* = G \times v_{termc} \tag{19}$$

3 Simulation Results

The solar PV system connected to the grid is simulated in MATLAB along with Simulink toolbox. The simulation results of grid side voltage (V_{grid}), grid side current (I_{grid}), DC link voltage (V_{dc}), load current (I_{la}, I_{lb}, I_{lc}), PCC current (I_{pa}, I_{pb}, I_{pc}), PV voltage (V_{pv}), PV current (I_{pv}), and PV power (P_{pv}) for different algorithms are shown in Figs. 2 and 3. Nonlinear load (universal bridge with 10 Ω, 100 mH) is used. Due to nonlinearity, THD of load current is 10.96 %. Simulation for different algorithms are performed taking into consideration the standard test condition of 1000 W/m^2 and 25 °C.

For performance under transient conditions, load unbalancing is introduced at 0.3–0.45 s. As seen from the figures, for all the algorithms V_{dc} remains constant and PCC voltage is regulated. A comparative analysis THD level of PCC voltage and grid current are presented in Table 1, which are well within IEEE limits [10].

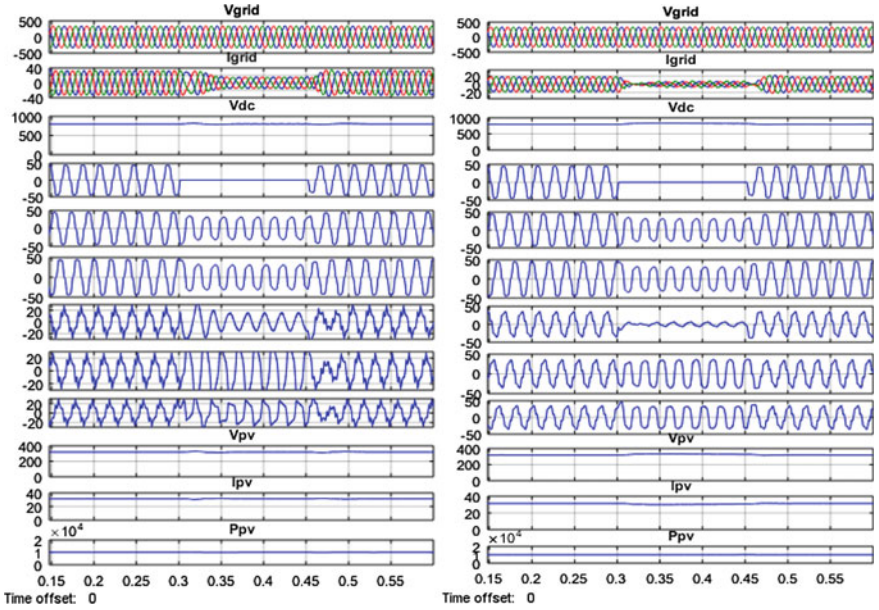

Fig. 2 Performance of SRF and unit template-based controller

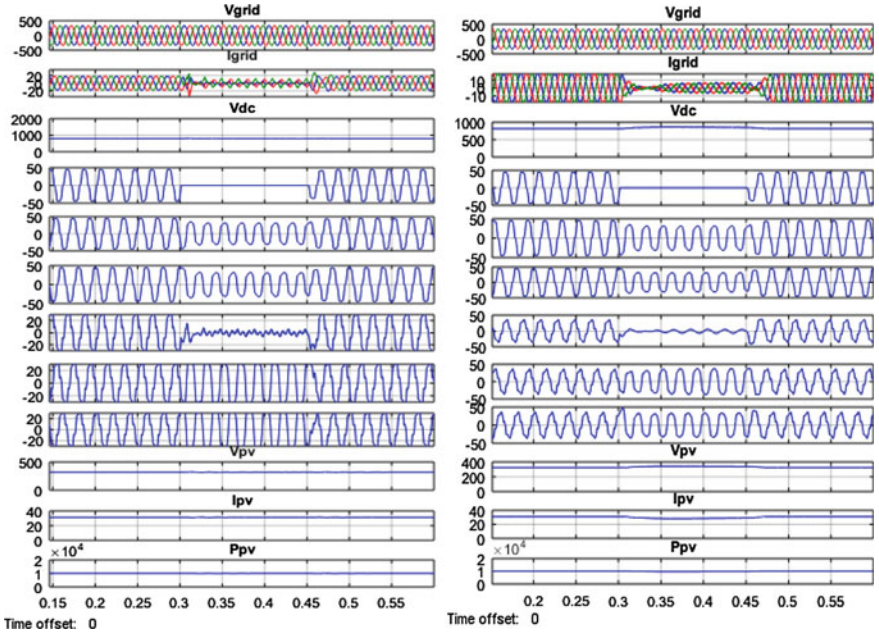

Fig. 3 Performance of IRP and conductance Fryze-based controller

Table 1 Performance of different algorithms under condition of load change

S. no.	Algorithm	Under load unbalancing		Under load increase	
		THD (%) of PCC voltage	THD (%) of supply current	THD (%) of PCC voltage	THD (%) of supply current
1	SRFT	3.07	2.37	2.56	6.90
2	Unit template	2.41	3.12	2.04	4.98
3	IRPT	3.02	2.52	2.42	7.00
4	Conductance Fryze	1.49	2.03	1.59	4.68

4 Conclusions

This paper presents four conventional control algorithms for control of PV inverter to integrate PV module with microgrid. The mathematical analysis of the four algorithms, i.e., SRFT, unit template, IRPT, and conductance Fryze have been presented to demonstrate the behavior of PV inverter. Conductance Fryze control algorithms have been found most suitable among all discussed algorithms. PCC and DC bus voltages of the PV inverter have also been regulated to reference values under all load conditions.

References

1. McEvoy A., Markvart T., Castaner L.: Practical Handbook of Photovoltaics-Fundamentals and Applications. 2nd ed. Wyman Street, USA: Elsevier (2012).
2. Rub H.A., Malinowski M., Al-Hadad K.: Power electronics of renewable energy systems, transportation, and industrial application. 1st ed. United Kingdom: IEEE press and John Wiley and Sons publication (2014).
3. Singh B., Chandra A., Al-Haddad K.: Power Quality: Problems and Mitigation Techniques. United Kingdom: John Wiley & Sons (2014).
4. Singh B., Solanki J.: A Comparison of Control Algorithms for DSTATCOM. IEEE Transaction on Industrial electronics, vol.56 no. 7 (July 2009).
5. Gupta N., Garg R., Kumar P.: Characterization Study of PV module Connected to Microgrid. In: Proceedings of the IEEE India International Conference JMI, India. (Dec. 2015).
6. Verma A.K., Singh B., Sahani D.T.: Grid Interfaced Photovoltaic power generating system with Power Quality Improvement at AC mains. In: Proceedings of the IEEE Third International Conference on Sustainable Energy Technologies (ICSET), Kathmandu (Sept. 2012).
7. Singh B., Kumar S.: Modified Power Balance Theory for Control of DSTATCOM. In: Proceedings of the Joint International Conference on Power Electronics, Drives and Energy Systems (PEDES) & 2010 Power India, New Delhi (Dec. 2010).
8. Hirofumi A., Edson W., Aredes M.: Instantaneous power theory and applications to power conditioning. 1st Ed. New Jersey: IEEE Press-Wiley Press Pvt. Ltd. (2007).
9. Rowey C.N., Summersz T.J., Betz R.E., Cornforth D.: A Comparison of Instantaneous and Fryze Power Calculations on P-F and Q-V Droop in Microgrids. In: Proceedings of the 20th Australasian Universities Power Engineering Conference, Christchurch (Dec. 2010).
10. IEEE Recommended Practices and Requirements for Harmonics Control in Electric Power Systems, IEEE Standard 519 (1992).